ZESZYTY ENERGETYCZNE
TOM IV. *Modelowanie procesów cieplno-przepływowych*
2017, s. 51–62

Numerical modelling of ejector operating with isobutane

Kamil Śmierciew[1], Dariusz Butrymowicz[1], Jerzy Gagan[1], Sławomir Pietrowicz[2]

[1] *Białystok University of Technology, Faculty of Mechanical Engineering Division of Heat Technology and Refrigeration*
[2] *Wrocław University of Science and Technology, Faculty of Mechanical and Power Engineering, Department of Thermodynamics, Theory of Machines and Thermal Systems*
E-mail: slawomir.pietrowicz@pwr.edu.pl

ABSTRACT

The rapid growth of various applications of the ejection refrigeration systems could be observed recently. Because of possibility of the application of solar or waste energy to supply the motive energy they can be thought as a real alternative to compression devices in air-conditioning technologies. Ejection system can effectively compete with absorption system under temperature of the motive heat source lower than 80°C. The paper deals with CFD numerical simulation along with experimental investigations carried out on a specially constructed prototype/stand for the case of isobutane as a working fluid under motive vapour temperature below 75°C. The numerical and experimental results of entrainment ratio were compared. A good accuracy between numerical and experimental results was observed. The divergent of the results are lower than 20% for tested series. The exemplary pressure and velocity field were presented. Also it was shown that predicted by numerical simulation pressure distribution at ejector wall fits well with experimental pressure distribution.

KEYWORDS: *isobutane, numerical, modeling*

1. INTRODUCTION

Buildings represent a very high energy consumption percentage compared to other economy sectors. Although percentages vary from country to country, buildings are responsible for about 30-45$\%$ of the global energy demand. Residential air-conditioning and refrigeration consumes over 21% of electric energy used for household purposes.

Compressors use an average of 70% of the energy consumed by heating, ventilation, air-conditioning, and refrigeration systems. Air-conditioning creates also two sources of environmental pollution: the first one is direct emission of greenhouse gases, especially for working fluids belonging to HFC group, and the second one is emission of the greenhouse gases during generation of electric power to drive the system. Both sources are contributing significantly to the global warming effect. The building sector, therefore, plays a significant role in mitigating the impacts of climate change through reducing the demand; i.e. energy conservation, and by maximising the use of renewable energy. This has increased the need for new energy substitutes and conversion methods to meet an increasing energy demand and pave the way to cost-effective heating and cooling solutions.

Paper presents development of air-conditioning technology that reduces the greenhouse gases emission by using natural refrigerants and also dramatically reduces the need for the electric power. This is accomplished by using free or inexpensive low temperature heat source, either solar or waste heat, as the main source of energy instead of electricity. Ejection refrigeration system (Fig. 1) is a modification of a well-known vapour compression cycle.

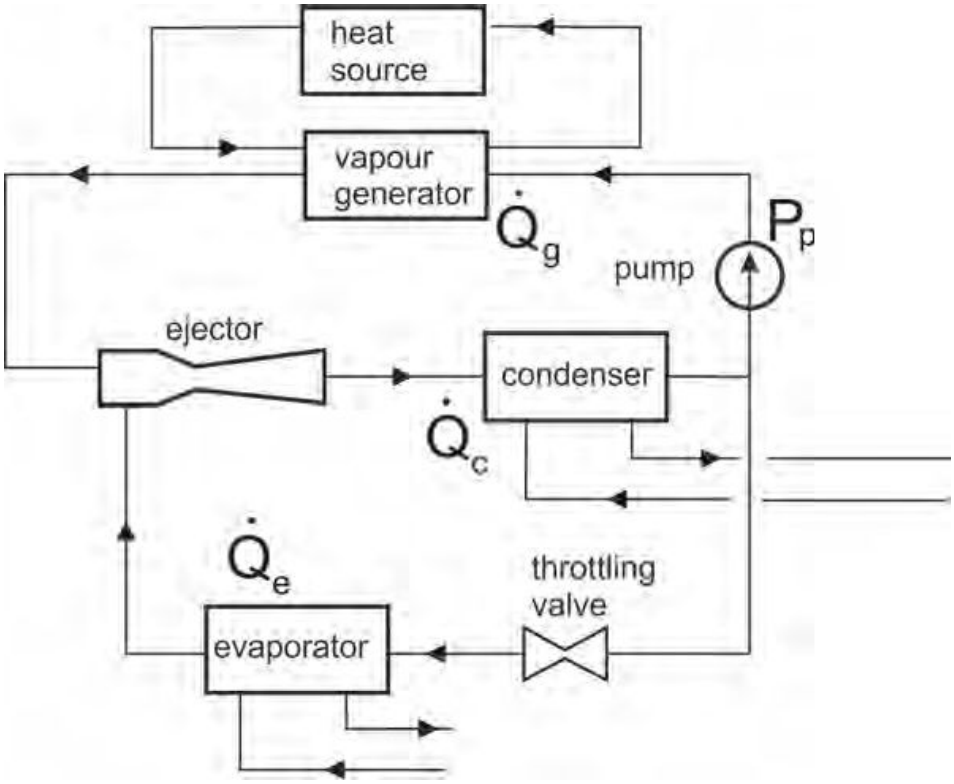

Fig. 1: Schematic of ejection refrigeration system: Q_g - motive heat, Q_e - cooling capacity, Q_c - condenser capacity

Instead of the refrigerant is not pressurized by a mechanical compressor, but by means of gas ejector. The gas ejector compresses refrigerant vapour flowing from evaporator and discharges it to the condenser. The motive vapour is generated in the vapour generator which is heated by low-temperature heat source. This low temperature heat source is the third heat source in refrigeration cooling cycles. Other two heat sources are exactly the same as in classic vapour refrigeration cycles. These three heat sources have

different temperatures: the vapour generator level, which is the temperature of the solar or waste heat source, a condensation level, which is the ambient temperature (actually this is a heat sink) and the evaporation temperature required for desirable cooling effect. The basic parameters describing the ejection cycle performance are mass entrainment ratio, eq. (1), and compression ratio, eq. (1):

$$U = \frac{\dot{m}_e}{\dot{m}_g} \tag{1}$$

$$\Pi = \frac{p_c - p_e}{p_g - p_e} \tag{2}$$

where: p_c is condensation pressure, p_e is evaporation pressure, p_g is saturation pressure in the vapour generator, and $\dot{m}_g$, $\dot{m}_e$ are the primary (motive) and the secondary fluid mass flow rates, respectively. The performance of the ejector depends on several quantities such as: operating pressures and temperatures at the ejector inlets and outlet, working fluid properties and ejector geometry. The performance of the ejector depends on several quantities such as: operating pressures and temperatures at the ejector inlets and outlet, working fluid properties and ejector geometry. Many research teams have numerically and experimentally investigated the performance of the ejector cycle for various working fluids and operating parameters, e.g. [1-3].
The efficiency of the ejector as a function of the ejector geometry were numerically as well as experimentally tested by several research teams, e.g. [4-8]. The state-of-art in the field of ejector investigations is presented in authors previous paper Butrymowicz et al. [9].

This paper deals with own experimental and numerical investigation of supersonic vapour ejector operating with isobutane as a working fluid in an ejection air-conditioning systems driven by low-temperature heat source. Selection of the working fluid for the solar air-conditioning system was based on the analysis of the energy efficiency of the system presented by Butrymowicz et al. [9] for the following fluids: isobutane, ammonia, propane, methanol, water. Results of this shown that isobutane is the best option as a working fluid for ejection system in application to air-conditioning since it offers the highest COP.

The exemplary results of the investigation of isobutane ejector were presented in the paper. The investigation covers the on-design and off-design operating regime of the ejector. The ejector operates at on-design condition in the case of choked both streams: primary (motive) stream and secondary stream. This operating regime covers the back pressure which is corresponding to the condensation pressure smaller than the some specific value of the pressure called the critical pressure p_c. At this regime the ejector entrains the maximum amount of vapour from the evaporator, and the mass entrainment ratio U is constant. The critical pressure depends on the ejector geometry and the inlet parameters at the both inlets of the ejector. The back-pressure higher than the critical pressure p_c makes the ejector starts to operate at the off-design condition. At this operating regime the secondary flow is not choked already and the mass entrainment ratio U decreasing with increasing of the back-pressure.

The assessment of the performance of the ejector as relationships between mass entrainment ratio and condensation temperature is presented in the paper. The experimental results are compared with numerical simulation obtain from CFD code.

2. Apparatus and methodology

The experimental rig presented in Fig. 2 was build and instrumented for operation with isobutane. The main elements of the rig are listed in the figure caption. The geometry of the test ejector is presented in Fig. 3. The motive nozzle throat diameter was 3.5 mm. The testing stand was equipped with the temperature sensors and pressure transducers installed at the critical locations and other locations of interest. The pressure sensors of the measurement accuracy class 0.1 and the flow-meters of the measurement accuracy class 0.5 were used during the experiments. First-class K-type thermocouples were applied for the experiments.

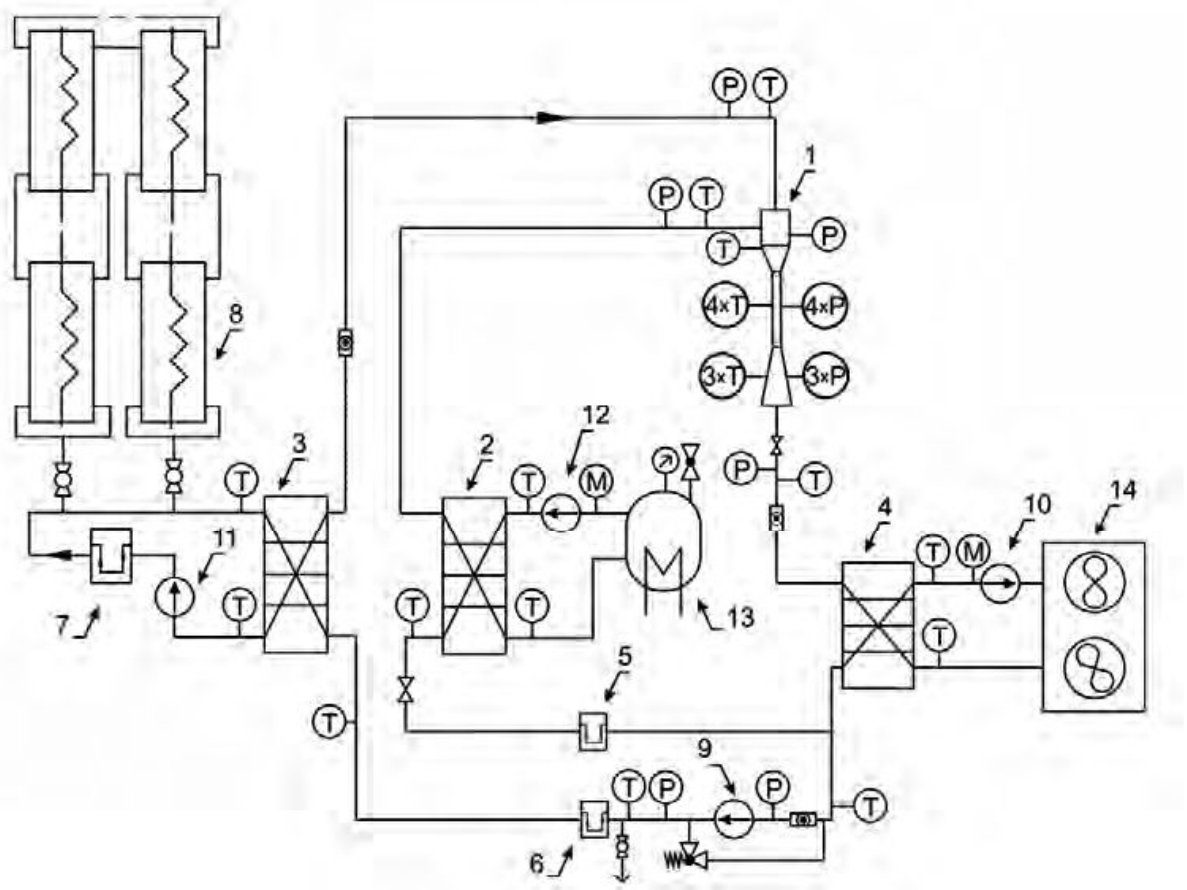

Fig. 2: Schematic of testing stand: 1 – tested ejector; 2 – evaporator; 3 – vapour generator, 4 – condenser refrigerant pump; 5, 6, 7 – mass flow meters; 8, 13 – electric heaters; 9 – circulation pump; 10 – circulation pump in condenser cooling loop; 11 – circulation pump in evaporator heat load loop; 12 – circulation pump in evaporator heat load loop, 14 - dry cooler; T – temperature sensor; P – pressure transducers; M – mass flow meters in cooling/heating loops

The test rig was equipped with two additional loops: the first for the thermal load for the evaporator and the second for the condenser cooling. These systems allow for adjusting refrigerant flow rates as well as for changing of operation parameters in the wide range. The condenser cooling system was equipped with an automatically controlled dry cooler. The thermal load system was equipped with automatically controlled electrical heater. Both systems are fully instrumented with transducers for measuring temperatures, pressures and flow rates with high accuracy. The rig is equipped with control valves enabling the adjustment of the operating parameters of the motive vapour at the inlet to the motive nozzle of the ejector.

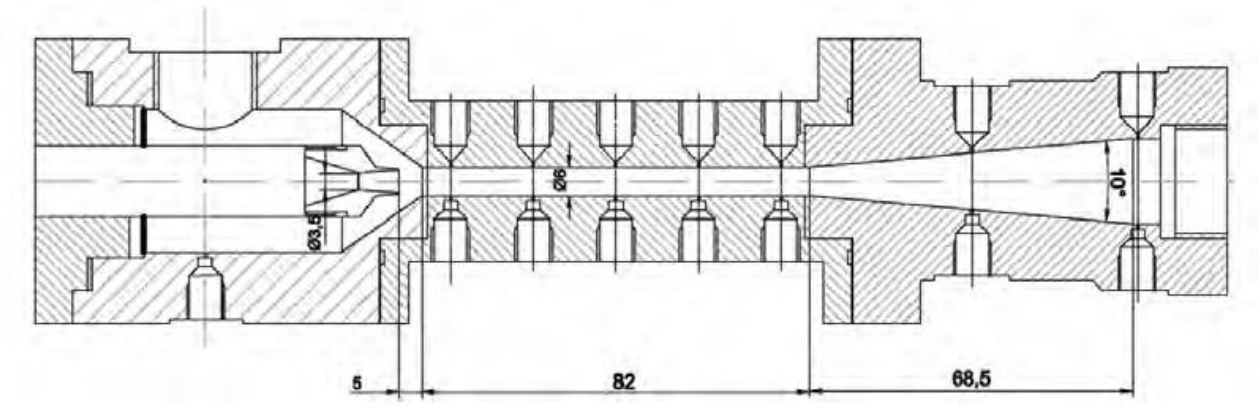

Fig. 3: Schematic of tested ejector; unit: mm

Table 1: Operating parameters

No.	Series No.	High pressure inlet		Low pressure inlet		Outlet		Conden. temp.
		temp.	pres.	temp.	pres.	temp.	pres.	°C
		°C	bar	°C	bar	°C	bar	
1	Series No.1	65,80	8,29	13,07	1,97	27,36	3,75	27,36
2		66,15	8,32	13,23	1,98	27,95	3,82	27,95
3		65,58	8,29	13,10	1,97	28,28	3,85	28,28
4		66,19	8,31	13,49	2,00	29,03	3,94	29,03
5		65,67	8,24	13,56	1,97	29,50	3,99	29,50
6		66,36	8,33	13,45	1,95	29,84	4,03	29,84
7		66,23	8,30	14,09	1,95	30,00	4,04	30,00
8		65,56	8,30	14,10	1,95	31,14	4,06	30,14
9		66,33	8,33	14,12	1,93	30,23	4,07	30,23
10	Series No.2	63,94	7,75	10,68	1,82	24,03	3,41	24,03
11		62,49	7,79	10,81	1,84	24,50	3,45	24,50
12		62,62	7,77	11,23	1,85	24,75	3,48	24,75
13		62,86	7,76	11,18	1,84	26,06	3,61	26,06
14		63,22	7,78	11,14	1,83	26,64	3,68	26,64
15		62,86	7,72	11,39	1,83	27,20	3,74	27,20
16		62,94	7,74	11,92	1,85	27,82	3,80	27,82

Generally, the performance of the ejector was changed by means of adjusting the mass flow rate of the coolant in the condenser loop. As an effect the condensation temperature was varying. In present investigations saturation pressure in the generator, superheating, volume flow rate and temperature of the motive primary vapour were kept constant. Also the evaporation pressure, temperature and superheating of the secondary stream were kept constant. The average operating parameters are listed in Table 1. It is worth to note that data collected in Table 1 corresponding only to conditions used in numerical calculations. The experimental data for each series contain more measuring point, which are not presented here.

3. Numerical simulation

Computational Fluid Dynamics (CFD) is widely use in simulation of the ejector performance, e.g. investigation of the influence of the operating conditions [10, 11] or type of working fluid [7, 12]. CFD technique is also used in geometry improvement or

optimization [5, 6, 8]. For CFD modelling of the ejector the 3-D model was applied. For mesh independent test three types of grid were prepared. For mesh No. 1 the ejector geometry was divided into three domain: motive nozzle, suction chamber, and mixing chamber with diffuser. Each domain was discretised with unstructural tetragonal mesh build in ICEM CFD and merged in ANSYS CFX using Interface boundary conditions. The total mesh density was 2×10^6 cells.

Fig. 4: Part of numerical model with mesh: suction and mixing chambers (left); motive nozzle (right)

Mesh No.2 was built as one domain with unstructural tetragonal cells and refined using grid adaptation tools to detect the anticipated local effects such as shockwave propagation and the boundary layer effect. The final grid density was 1.5×10^6 cells after mesh adaptation. Mesh No. 3 was generated analogically as mesh No. 2, however, with smaller dimensions of cells. After adaptation the grid density was 4.5×10^6 cells. Part of numerical mesh No. 1 before adaptation is shown in Fig. 4.

For modelling of the gas ejector the turbulence model from $k-\epsilon$ or $k-\omega$ group are commonly used [13, 14]. Therefore in initial simulation the standard $k-\epsilon$, realizable $k-\epsilon$, standard $k-\omega$ and SST $k-\omega$ turbulence models have been tested [15, 16]. Pressure distribution along ejector wall predicted by tested turbulence models were compared with experimental pressure distribution in order to choose most accurate turbulence model. Finally, the SST (Shear Stress Transport) turbulence model from $k-\omega$ group was applied. The boundary conditions used in simulations are the same as the operation parameters described in Table 1. Pressure boundary conditions were applied in the calculations with discretization of the second order. For high and low pressures inlets the temperature and pressure are set, while for ejector outlet only the pressure was set as boundary condition, according to Table 1. The pressure-velocity coupled solver was used and the convergence of residua 10^{-6} was assumed in the calculations. The thermodynamic properties of fluid from NIST REFPROP were applied in simulations.

4. Results of investigation

First step in numerical modelling was mesh independence test. An exemplary operating conditions (point No. 3 from series No. 1 in Table 1) were chosen for test simulation. The mass flow rate for both fluid were observed and compared with experimental values. The pressure distribution along ejector was also observed and compared

Table 2: Mass flow rate for tested meshes

Parameter	Unit	Experiment	Mesh No.1	Mesh No.2	Mesh No.3
$\dot{m}_g$	kg/s	0,026970	0,029303	0,028705	0,032036
$\dot{m}_e$	kg/s	0,005089	0,009376	0,010244	0,005846
$\dot{m}_e/\dot{m}_g$	-	0.189000	0,320000	0,357000	0,182000

to experimental. Results of mass flow rates are presented in Table 2. Based on the results presented in Table 2 it is seen that the numerical results obtain from simulation with mesh No. 3 is most accurate with experimental value.

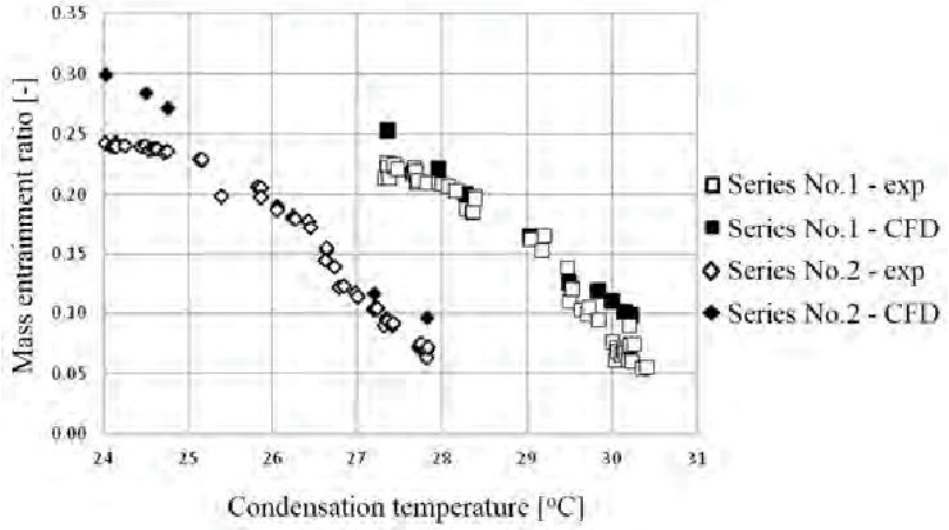

Fig. 5: Performance of the tested ejector: mass entrainment ratio vs. condensation temperature

Mass entrainment ratio as the function of the condensing temperature tc for tested ejector was shown in Fig. 5. Both, numerical and experimental results have been presented. For series No. 1 mean value of saturation temperature corresponding to the motive pressure is 58°C while mean motive temperature at saturation condition for series No. 2 is 55°C. The results clearly shows that for higher motive temperature /pressure the ejector can operate at higher condensation temperature. It is seen that for both series the numerical results in most cases fits well with experimental results. The deviation between numerical and experimental results of mass entrainment ratio are shown in Fig. 6 for Series No. 1 and in Fig. 7 for Series No. 2.

The figures shows that for both tested series, the deviation is lower than 20% for most of the numerical results. However it can be seen that numerical simulation overpredicts the mass entrainment ratio. This feature of the numerical simulation can result from omitting the flow resistance of the secondary flow and simplification of the suction chamber inlet. As a results of lack of flow resistance the velocity of the secondary vapour sucked by ejector is higher, the amount of the secondary fluid increase and therefore the ejector operate with higher entrainment ratio.

Figure 8 presents CFD results of the pressure and velocity profile along the ejector. As seen in Fig. 8 (top), the pressure of the primary flow is equal to 8.3 bar, which drastically decreases after the nozzle throat where the flow is supersonic. The supersonic flow creates a low pressure region (0.6 bar) which can suck the secondary flow into the ejector. They mix in the mixing chamber and the pressure is then recovered once in the mixing chamber is approximately 4 bar and afterward it will again increase

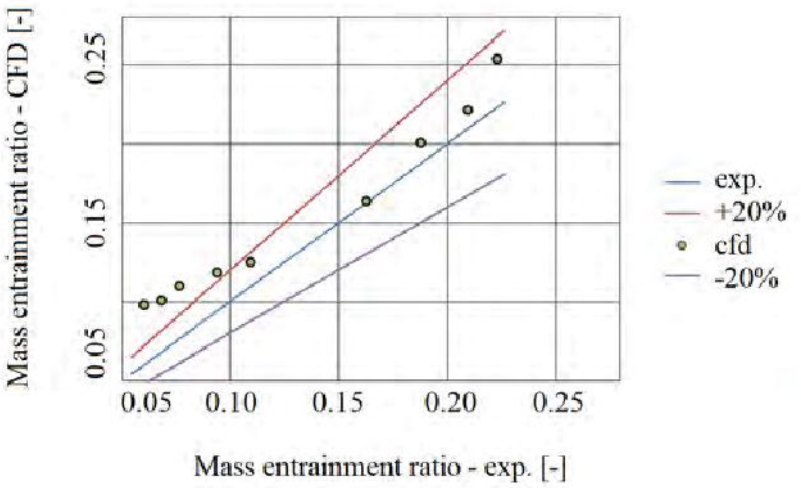

Fig. 6: Deviation of the numerical results for Series No. 1

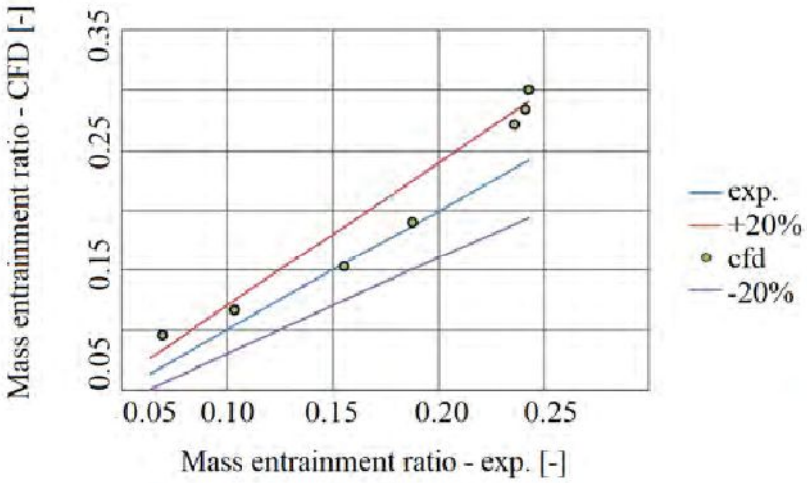

Fig. 7: Deviation of the numerical results for Series No. 2

in the beginning of the diffuser section to 4.46 bar. The velocity contours are shown in Fig. 8 (bottom). The velocity of the primary flow gradually increases as it passes through the nozzle and it reaches to its maximum value (around 390 m/s, corresponding to Mach number $Ma \approx 2.0$) at the nozzle outlet where the pressure is minimal. It can also be seen that the flow velocity gradually decreases to approximately 200 m/s in the mixing chamber as well as the diffuser by increasing the pressure. Finally, a uniform velocity profile of the primary and the secondary mixtures can be observed at the outlet section where the velocity is relatively low. Presented flow field is typical for off-design operating regime of the ejector without normal shock wave.

Figure 9 illustrates the comparison between the static pressure distributions from the two different approaches, the experimental versus the simulated results. The comparison was conducted when the ejector was operated at downstream pressure corresponding to t_c = 27.3°C. As seen in Fig. 9 the pressure profile fits well, however numerical values of pressure after shock wave are over-predicted. It is possible that this is an effect of the simplification of the ejector geometry. It is worth to note, that during experiments the ejector was equipped with pressure transducers and temperature sensors which have a negative influence on the flow of the refrigerant due to flow resistance and pressure

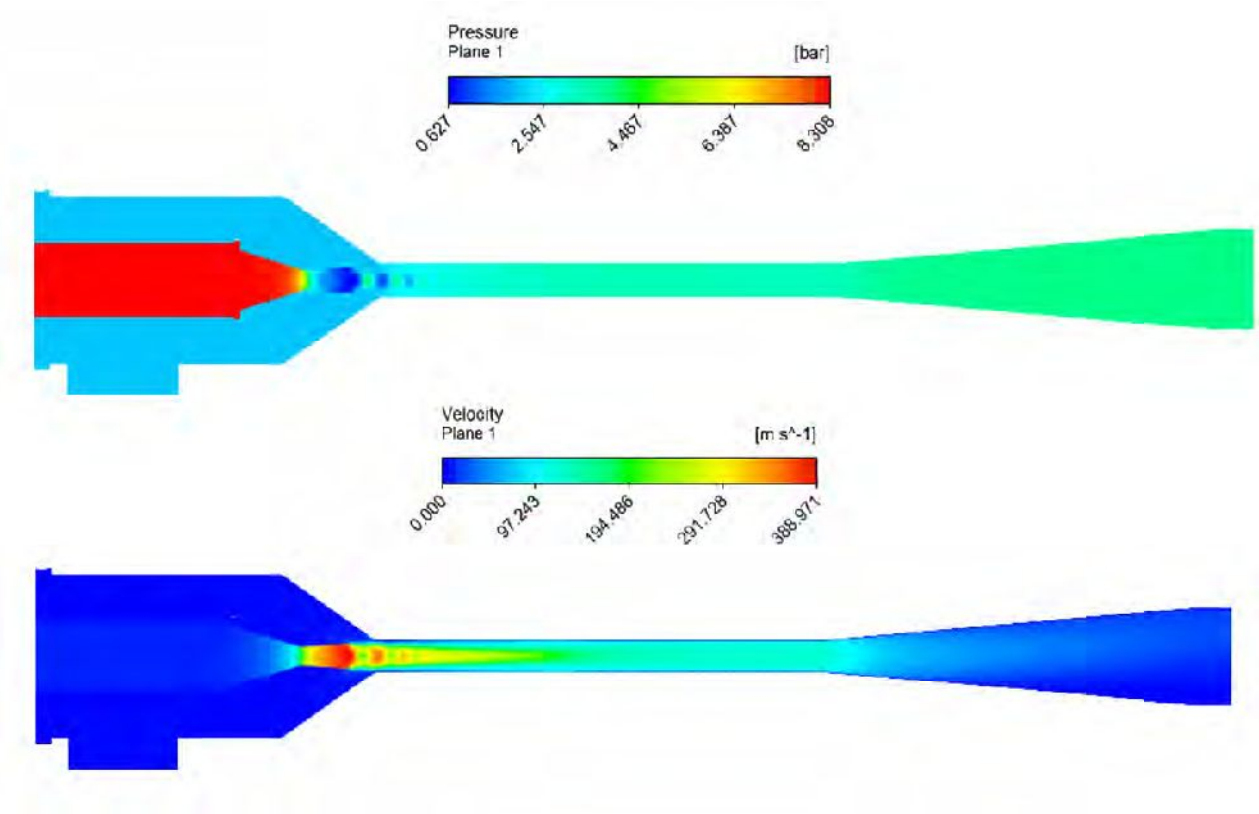

Fig. 8: Pressure (top) and velocity (bottom) filed in tested ejector for Series No. 1 and condensation temperature t_c = 30°C

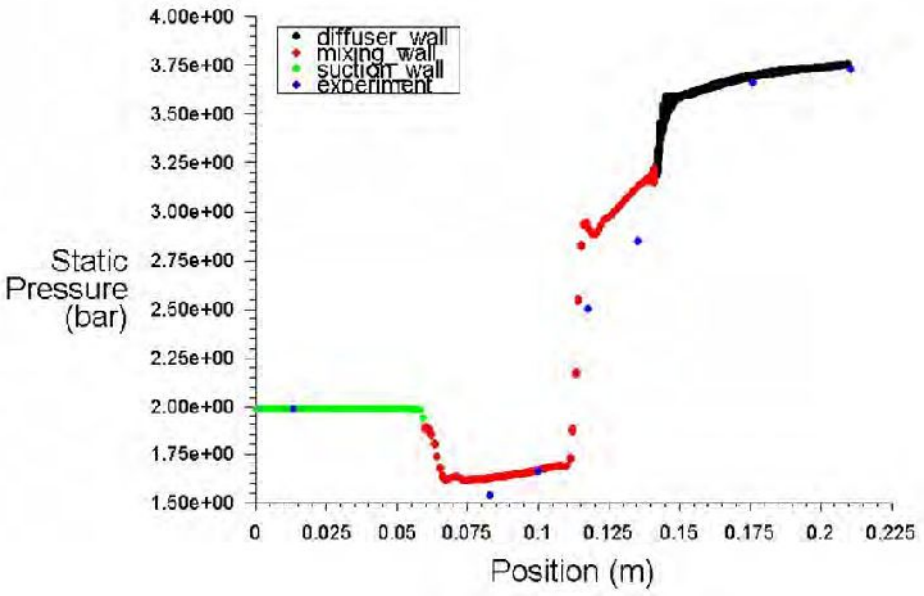

Fig. 9: Pressure distribution along ejector wall for Series No. 1 (point No. 1) and condensation temperature t_c = 27.3°C

and velocity losses. These sensors are not included in the numerical simulation, therefore, all effects caused by these sensors were omitted. Nevertheless, in general a good agreement between numerical and experimental pressure profile is observed.

In order to better understand ejector operation the authors undertook a very ambitious task, i.e. the use of LES model (Large Eddy Simulation) for gas ejector. In

following figures the exemplary preliminary results are shown. Velocity field profile is shown in Fig. 10. The largest difference in reference to results of 3D DNS (Direct Numerical Simulation) simulation shown in Fig 8 are for diffuser. Not symmetrical vortexes in diffuser are clearly seen in Fig. 10. Also, the supersonic jet in mixing chamber in larger in LES simulation.

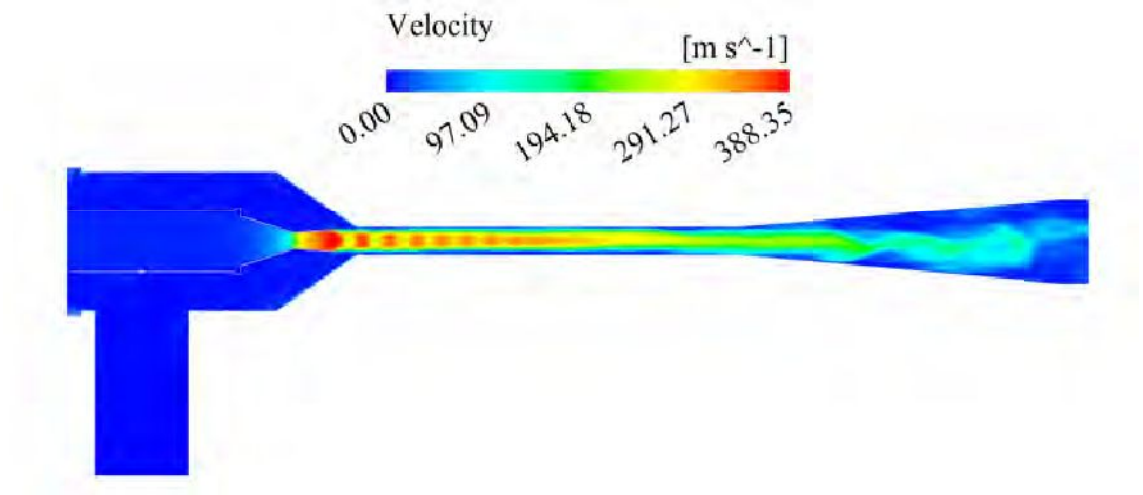

Fig. 10: Velocity field in modeled ejector

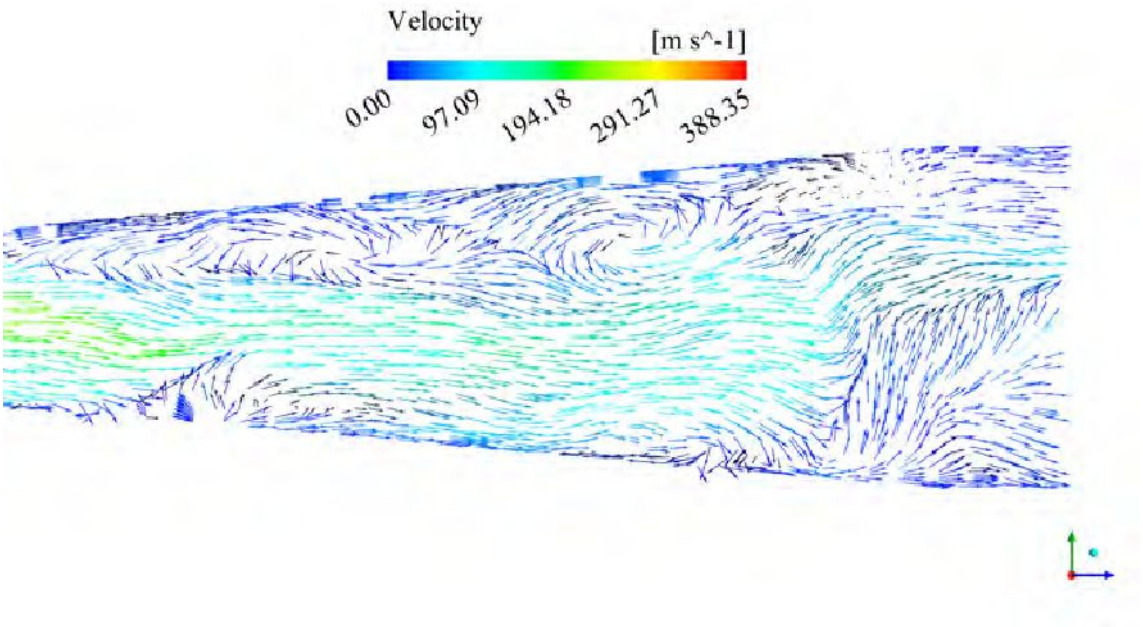

Fig. 11: Velocity vectors in diffuser

Enlarged views of velocity vectors in ejector are given in Fig. 11 and Fig. 12. Not symmetrical jet in mixing chamber is seen and also vortexes in diffuser and in suction chamber. Difference in supersonic jet in mixing chamber between LES and DNS simulation might have negative influence on proper interpretation of results, especially during ejector design and determination of critical temperatures at which ejector regime is changing from on-design to off-design.

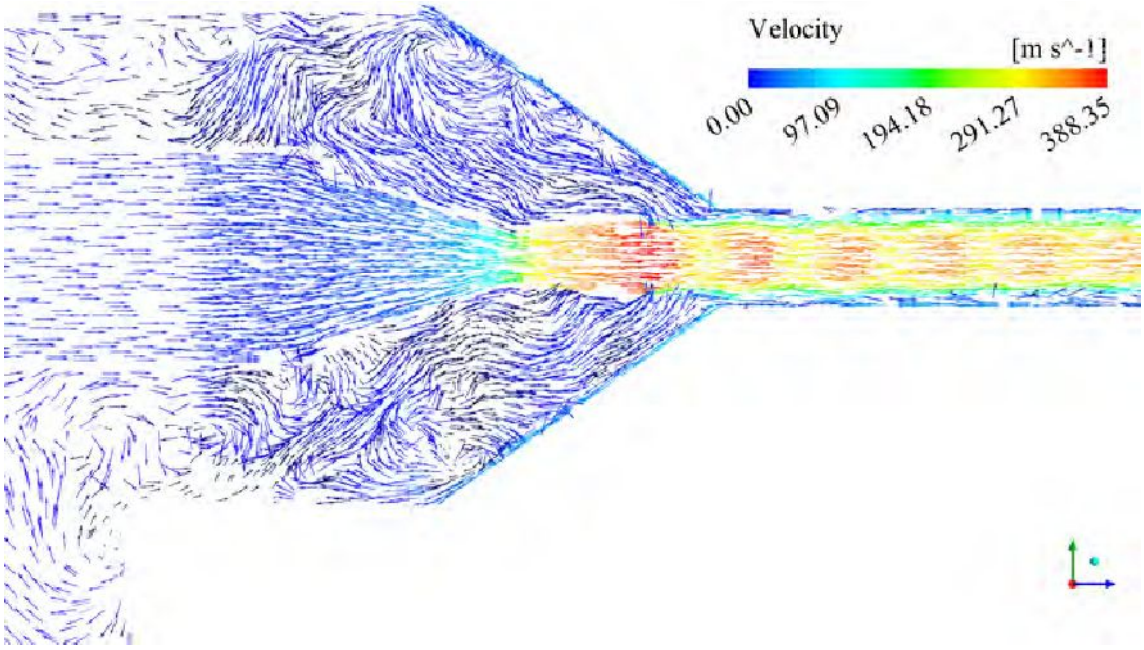

Fig. 12: Velocity vectors in nozzle, suction and mixing chambers

5. Conclusions

The own experimental and numerical investigation of the ejection system driven by low-temperature source have been shown. The experimental investigations confirmed that the ejection cycle operating with isobutane can effectively be driven by low temperature heat source, e.g. lower that 75°C. Under this range of motive temperature heat sources the ejection cycles can be considered as truly competitive in comparison with absorption refrigeration systems. It was also shown that for higher value of the motive vapour the ejector operates at higher values of the condensation temperature. Based on the numerical results it can be concluded that the CFD method is an efficient tool to predict the entrainment ratio and pressure profile. In general, it can be concluded that chosen turbulence model gives good representation of the flow inside ejector.

Acknowledgement

The work was completed within the statutory activities S/WM/2/2016. Also the work was partly supported by Wroclaw Centre for Networking and Supercomputing WCSS (http://wcss.pl) in the scope of Grant No. 309.

References

[1] Pridasawas W., Lundqvist P., *Natural working fluids for a solar-driven ejector refrigeration system*, Proceedings of the Eurotherm Seminar No. 72, Thermodynamics, Heat and Mass Transfer of Refrigeration Machines and Heat Pumps, 431-436, 2003.

[2] Butrymowicz D., Trela M., Karwacki J., Ochrymiuk T., Smierciew K., *Investigation and modelling of ejector for air-conditioning system*, Archives of Thermodynamics, **29**, 27-40, 2008.

[3] Śmierciew K., Butrymowicz D., Karwacki J., Trela M., *Modelling of ejection cycle for solar air-conditioning*, Proceedings of the International Seminar on ejector/jet-pump technology and application, **25**, 2009.

[4] Zhu Y., Cai W., Wen C., Li Y., *Numerical investigation of geometry parameters for design of high performance ejectors*, Applied Thermal Engineering, **29**, 898–905, 2009.

[5] Utomo T., Ji M., Kim P., Jeong H., Chung H., *CFD analysis on the influence of converging duct angle on the steam ejector performance*, Proceedings of the International Conference on Engineering Optimization EngOpt, 2008.

[6] Dvořák V., *Shape optimization of axisymmetric ejector*, Proceedings of the European Conference on Computational Fluid Dynamics, 2006.

[7] Eames I.W., Ablwaifa A.E., Petrenko V., *Results of an experimental study of an advanced jet-pump refrigerator operating with R245fa*, Applied Thermal Engineering, **27**, 2833–2840, 2007.

[8] Varga S., Oliviera A.C., Diaconu B., *Influence of geometrical factors on steam ejector performance – A numerical assessment*, International Journal of Refrigeration, **32**, 1694-1701, 2009.

[9] Butrymowicz D., Śmierciew K., Karwacki J., Gagan J., *Experimental investigations of low-temperature driven ejection refrigeration cycle operating with isobutane*, International Journal of Refrigeration, **39**, 196-209, 2014.

[10] Hemidi A., Henry F., Leclaire S., Seynhaeve J.M, Bartosiewicz Y., *CFD analysis of a supersonic air ejector. Part II: Relation between global operation and local flow features*, Applied Thermal Engineering, **29**, 2990-2998, 2009.

[11] Sriveerakul T., Aphornatana S., Chunnanond K., *Performance prediction of steam ejector using computational fluid dynamics: Part 2. Flow structure of a steam ejector influenced by operating pressures and geometries*, International Journal of Thermal Sciences, **46**, 823-833, 2007.

[12] Yapici R., *Experimental investigation of performance of vapour ejector refrigeration system using refrigerant R123*, Energy Conversion and Management, **49**, 953–961, 2008.

[13] Bartosiewicz Y., Aidoun Z., Desevoux P., Mercadier Y., *CFD-Experiments Intergation in the evaluation of Six Turbulence Models for Supersonic Ejector Modeling*, Proceedings of the Conference on the Integrating CFD and Experiments, 2003.

[14] Gagan J., Śmierciew K., Butrymowicz D., Karwacki J., *Comparative study of turbulence models in application to gas ejectors*, International Journal of Thermal Sciences, **78**, 9-15, 2014.

[15] Menter F.R., Kuntz M., Langtry R., *Ten Years of Industrial Experience with the SST Turbulence Model, In: Hanjalic K. et al.*, Turbulence, Heat and Mass Transfer, 2003.

[16] Kolar J., Dvorak V., *Verification of k-omega SST turbulence model for supersonic internal flows*, World Academy of Science, Engineering and Technology, **81**, 262-266, 2011.